The Astrophysical Journal, 633:1187–1190, 2005 November 10

COMPARISON OF SOLAR CYCLE VARIATIONS OF SOLAR *p*-MODE FREQUENCIES FROM GONG AND MDI

Alexander Serebryanskiy
National Solar Observatory, Tucson, AZ 85719; and Ulugh Beg Astronomical Institute, Tashkent, Uzbekistan; alex@astrin.uzsci.net

and

Dean-Yi Chou
Institute of Astronomy and Department of Physics, National Tsing Hua University, Hsinchu, 30043, Taiwan; chou@phys.nthu.edu.tw
Received 2005 April 29; accepted 2005 July 20

ABSTRACT

The solar *p*-mode frequencies change with the solar cycle. The horizontal phase velocity dependence of the relative frequency change scaled by mode mass provides depth information on the perturbations in the solar interior. Both GONG data and *SOHO* MDI data show that the horizontal phase velocity dependence of the scaled relative frequency change varies with solar cycle. Temporal variations of GONG and MDI frequency changes are qualitatively consistent despite some discrepancies. For both GONG and MDI, the smoothed scaled relative frequency change versus horizontal phase velocity is approximately constant at small horizontal phase velocities, but its value decreases for horizontal phase velocities higher than a critical value, as surface activities develop. This critical horizontal phase velocity corresponds to a depth near the base of the convection zone. The magnitude of the decrease in frequency change at large horizontal phase velocities approximately correlates with the sunspot number for both GONG and MDI, although the GONG magnitude is greater than the MDI one. If these signals are real, it suggests that the wave speed in a region near the base of the convection zone changes with the solar cycle. This change might relate to solar cycle variations of magnetic fields near the base of the convection zone.

Subject headings: Sun: evolution — Sun: helioseismology — Sun: interior — Sun: magnetic fields

1. INTRODUCTION

Observations show that the solar *p*-mode frequencies vary with the solar cycle. The magnitude of frequency change correlates with magnetic activities (Libbrecht & Woodard 1990; Woodard et al. 1991; Rhodes et al. 1993; Regulo et al. 1994; Elsworth et al. 1994; Chaplin et al. 1998; Jimenez 2002; Howe et al. 2002; Jain & Bhatnagar 2003). It has been suggested that the measured frequency change is caused by changes in physical conditions near the surface (Libbrecht & Woodard 1990; Shibahashi 1991). Many attempts have been made to detect the solar cycle variations of structure deep in the solar interior with inversion of helioseismic data, but until now no evidence has been found (Howe et al. 1999; Basu & Schou 2000; Antia et al. 2001; Basu & Antia 2002; Eff-Darwich et al. 2002; Basu et al. 2003). It is expected that the perturbations in the solar interior have a rather small contribution to the frequency change, if it exists, because of the large β, the ratio of gas pressure to magnetic pressure. It is also reasonable to expect, based on the current dynamo theories, that the second largest contribution to the frequency change might be from the perturbation near the base of the convection zone (BCZ), because it is the seat of the dynamo.

A resonant *p*-mode is trapped and multiply reflected in a cavity between the surface and a layer in the solar interior. Different modes have different penetration depths (lower turning points). The penetration depth is determined approximately by the horizontal angular phase velocity w ($\equiv \omega/L = \omega/[l(l+1)]^{1/2}$, where ω is the angular frequency and l is the mode degree; Christensen-Dalsgaard et al. 1985). The greater w is, the deeper the penetration depth. A perturbation near the BCZ would influence different modes in different ways: the frequencies of the modes that can penetrate into the BCZ would be modified, while the modes that cannot penetrate into the BCZ would remain unaffected. Therefore, we expect that the effects of the BCZ perturbation on the mode frequency would depend on w. The observed frequency change versus w provides information on the perturbations in the solar interior. However, because of the small effects on the frequency change, it is difficult to detect the perturbations deep in the solar interior.

In the asymptotic theory, the relative frequency change scaled by mode mass E_{nl}, to the first order, can be split into two terms (Christensen-Dalsgaard et al. 1988),

$$\frac{\delta\omega_{nl}}{\omega_{nl}} E_{nl} \approx H_1(w) + H_2(\omega), \tag{1}$$

where $H_1(w)$, depending only on w, is caused by the perturbations in the whole solar interior, while $H_2(\omega)$, depending only on ω, is caused only by the near-surface perturbations. The w dependence of $H_1(w)$ provides depth information on the perturbations in the solar interior. However, $H_2(\omega)$ and the error of measured frequencies would cause scattering in the plot of $(\delta\omega_{nl}/\omega_{nl})E_{nl}$ versus w and make the identification of the weak w dependence of $(\delta\omega_{nl}/\omega_{nl})E_{nl}$ difficult. Chou & Serebryanskiy (2005, hereafter Paper I) have shown with modeling that the small w dependence of $(\delta\omega_{nl}/\omega_{nl})E_{nl}$, generated by the perturbation near the BCZ, could be detected with smoothed $(\delta\omega_{nl}/\omega_{nl})E_{nl}$. They have also shown that the w dependence of smoothed $(\delta\omega_{nl}/\omega_{nl})E_{nl}$ measured with the Michelson Doppler Imager (MDI) varies with solar cycle. The smoothed $(\delta\omega_{nl}/\omega_{nl})E_{nl}$ remains constant at small w, while its value at w greater than a critical value decreases with solar activity. This critical w corresponds to a depth near the BCZ.

The perturbations discussed here are the changes in interior structure over the solar cycle. There is evidence for variations of interior dynamics over the solar cycle in previous studies, for example, variations of differential rotation near the BCZ (Howe et al. 2000) and variations of meridional flows in the convection zone (Chou & Dai 2001; Chou & Ladenkov 2005).

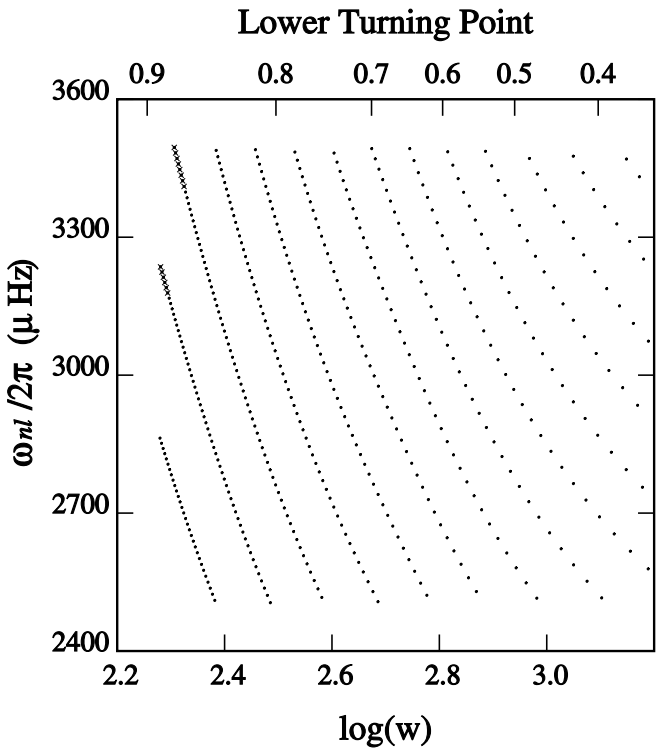

FIG. 1.—Distribution of modes used in this study in the $(\omega/2\pi, \log w)$-plane. There is no missing mode for the MDI frequency tables in the range of $2.5 \leq \omega/2\pi \leq 3.5$ mHz and $190 \leq w \leq 1570$. The crosses denote the missing modes in the GONG frequency tables.

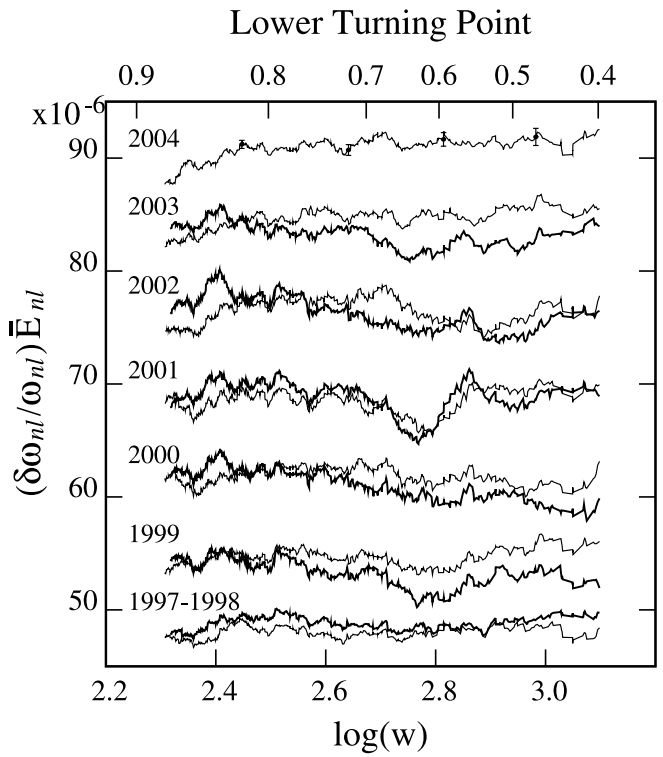

FIG. 2.—Smoothed $(\delta\omega_{nl}/\omega_{nl})\bar{E}_{nl}$ vs. $\log w$ for various periods along the solar cycle, using the frequency averaged over solar minimum (1996.05–1997.07) as the reference. The MDI result is denoted by the thin lines, and the GONG one by the thick lines. All periods are independent. The period of 1997–1998 is 1997.07–1998.10, which is also independent from the reference period. The curves of smoothed $(\delta\omega_{nl}/\omega_{nl})\bar{E}_{nl}$ are shifted vertically to avoid interference: 1997–1998 by 2.1×10^{-5}, 1999 by -1.5×10^{-5}, 2000 by -2.6×10^{-5}, 2001 by -1.9×10^{-5}, 2002 by -1.0×10^{-5}, 2003 by 3.6×10^{-5}, and 2004 by 6.2×10^{-5}. The MDI and GONG curves are shifted by the same amount. The error bars for the curve for MDI 2004 at $\log w = 2.45$, 2.64, 2.81, and 2.98 are the errors of the 41 point running mean, computed with the errors of the measured frequencies, based on the error propagation.

In this study, we apply the same analysis used in Paper I to the Global Oscillation Network Group (GONG) frequencies and compare its result with the MDI result. In § 2 we describe the data and their analysis. The comparison of GONG and MDI results is discussed in § 3.

2. DATA AND ANALYSIS

In this study, we use the solar *p*-mode frequencies derived from the data taken with MDI on board the *Solar and Heliospheric Observatory* (*SOHO*; Scherrer et al. 1995) and GONG (Harvey et al. 1996). To make a precise comparison for the frequencies from two projects, the data intervals selected from the two projects for comparison are identical. This is from 1996.05 (beginning of MDI data) to 2003.12. There are gaps for the MDI data in 1998 due to the problem with *SOHO*. The GONG data of these periods are excluded to make the data intervals of two projects consistent. The MDI frequencies are measured with a time series of 72 days (Schou 1999). All 72 day time series are independent in time; there is no overlap among them. The GONG frequencies are measured with a time series of 36 days. There is also no overlap among the 36 day time series. The 72 day MDI time series and the 36 day GONG time series are synchronized, so we could average the GONG frequencies over pairs of 36 day sets to bring them into line with the 72 day MDI sets. The frequencies derived from different time series are averaged over a period, for example, 1 yr, to increase the signal-to-noise ratio.

As in Paper I, the modes in the range of $2.5 \leq \omega/2\pi \leq 3.5$ mHz and $190 \leq w \leq 1570$ are used in this study. Here the value of w ($\equiv 2\pi\nu/L$) is computed with the frequency ν in units of μHz. There is no missing mode in this range for the MDI frequency tables, while there are 14 modes missing in this range for the GONG frequency tables, as shown in Figure 1. As discussed in Paper I, the missing modes would affect the smoothed frequency changes. However, the missing modes in the GONG frequency tables are located at $\log w < 2.33$, and they affect the smoothed frequency shifts only for $\log w < 2.37$. Therefore, they would not change the conclusion of this study.

The frequency averaged over a solar minimum period, 1996.05–1997.07, is used as the reference frequency. The frequency change $\delta\omega_{nl}$ along the solar cycle is computed relative to the reference frequency. The relative frequency change is scaled by the mode mass to obtain $(\delta\omega_{nl}/\omega_{nl})\bar{E}_{nl}$, where $\bar{E}_{nl}$ is the mode mass normalized by the mode mass of mode $n = 21$ and $l = 0$. The normalized mode mass $\bar{E}_{nl}$ is of the order of unity for the range of modes used in our study. The w dependence of $(\delta\omega_{nl}/\omega_{nl})\bar{E}_{nl}$ provides the depth information of perturbations. However, as shown in Paper I, $(\delta\omega_{nl}/\omega_{nl})\bar{E}_{nl}$ versus w is too scattered to see small variations of $(\delta\omega_{nl}/\omega_{nl})\bar{E}_{nl}$ versus w, if they exist. The model study in Paper I has shown that the small w dependence of $(\delta\omega_{nl}/\omega_{nl})\bar{E}_{nl}$ could be detected with smoothed $(\delta\omega_{nl}/\omega_{nl})\bar{E}_{nl}$. Here we smooth observed $(\delta\omega_{nl}/\omega_{nl})\bar{E}_{nl}$ with the 41 point box running mean to study the small variations of $(\delta\omega_{nl}/\omega_{nl})\bar{E}_{nl}$ versus w.

The smoothed $(\delta\omega_{nl}/\omega_{nl})\bar{E}_{nl}$ versus $\log w$ for different periods along the solar cycle is shown in Figure 2. All periods in Figure 2 are independent. Here $(\delta\omega_{nl}/\omega_{nl})\bar{E}_{nl}$ is plotted versus $\log w$ instead of w because the number of modes decreases quickly with w.

The MDI result is denoted by the thin line, and the GONG by the thick line. The curves of smoothed $(\delta\omega_{nl}/\omega_{nl})\bar{E}_{nl}$ are shifted to avoid interference. The MDI and GONG curves of each period are shifted by the same amount.

The error of the measured frequency of GONG is close to that of MDI. The error of each mode varies little along the solar cycle. To show the typical error of data in Figure 2, we plot the errors of four modes in the curve for MDI 2004 as examples. The errors of other periods for MDI are shown in Paper I. These errors are computed from the error propagation using the frequency errors quoted in the measured frequencies.

3. COMPARISON OF GONG AND MDI RESULTS

The MDI curves in Figure 2 are the same as those in Paper I, except the result for 2004 is added here. As described in Paper I, the interesting phenomenon for the MDI result is that the values of $(\delta\omega_{nl}/\omega_{nl})\bar{E}_{nl}$ at small w and large w are different: the w dependence of $(\delta\omega_{nl}/\omega_{nl})\bar{E}_{nl}$ varies with the solar cycle for $\log w > 2.7$, while it remains approximately constant for $\log w < 2.7$. In the period of low activity (1997–1998), the curve is approximately flat. As magnetic activity increases, the value of $(\delta\omega_{nl}/\omega_{nl})\bar{E}_{nl}$ at $\log w > 2.7$ becomes smaller relative to that at $\log w < 2.7$. The difference between small and large w increases with surface magnetic activity. The curve becomes approximately flat again in 2003 and 2004 as activity becomes low. The fact that the curve for 2004 is flat strengthens the finding in Paper I that variations of $(\delta\omega_{nl}/\omega_{nl})\bar{E}_{nl}$ at $\log w > 2.7$ correlate with magnetic activity. The phase velocity $\log w = 2.7$ corresponds to a lower turning depth near the BCZ. To quantify the drop at $\log w > 2.7$, we compute the difference between $(\delta\omega_{nl}/\omega_{nl})\bar{E}_{nl}$ averaged over $\log w = 2.45$–2.65 (small w) and $\log w = 2.7$–3.0 (large w), $\langle(\delta\omega_{nl}/\omega_{nl})\bar{E}_{nl}\rangle_{\rm large} - \langle(\delta\omega_{nl}/\omega_{nl})\bar{E}_{nl}\rangle_{\rm small}$. The magnitude of $\langle(\delta\omega_{nl}/\omega_{nl})\bar{E}_{nl}\rangle_{\rm large} - \langle(\delta\omega_{nl}/\omega_{nl})\bar{E}_{nl}\rangle_{\rm small}$ approximately correlates with the sunspot number, as shown in Figure 3. The value of $\langle(\delta\omega_{nl}/\omega_{nl})\bar{E}_{nl}\rangle_{\rm large} - \langle(\delta\omega_{nl}/\omega_{nl})\bar{E}_{nl}\rangle_{\rm small}$ would change if the ranges used to compute the averages over small and large w changed. However, the basic feature in Figure 3 that the magnitude of $\langle(\delta\omega_{nl}/\omega_{nl})\bar{E}_{nl}\rangle_{\rm large} - \langle(\delta\omega_{nl}/\omega_{nl})\bar{E}_{nl}\rangle_{\rm small}$ approximately correlates with the sunspot number remains unchanged. The yearly averages in Figure 3 are from independent data.

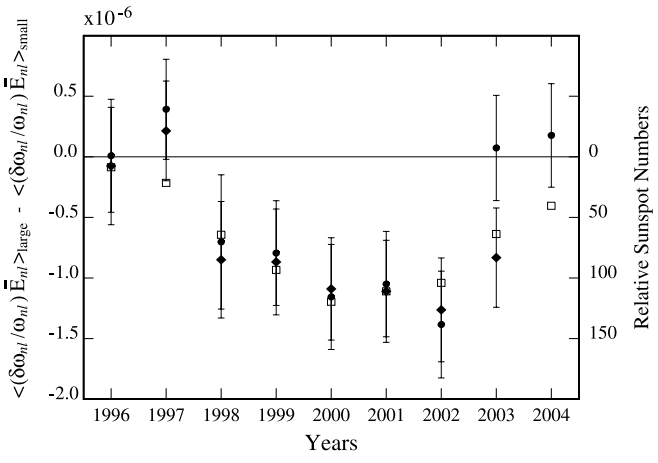

FIG. 3.—Difference between $(\delta\omega_{nl}/\omega_{nl})\bar{E}_{nl}$ averaged over large w ($\log w = 2.7$–3.0) and small w ($\log w = 2.45$–2.65) vs. time. The MDI result is denoted by the circle, and the GONG one by the diamond. It is noted that the value for GONG shown here is scaled by a factor of 2, but its error is not. The yearly averages shown here are from independent data. The relative sunspot number is denoted by the open square (van der Linden et al. 2005).

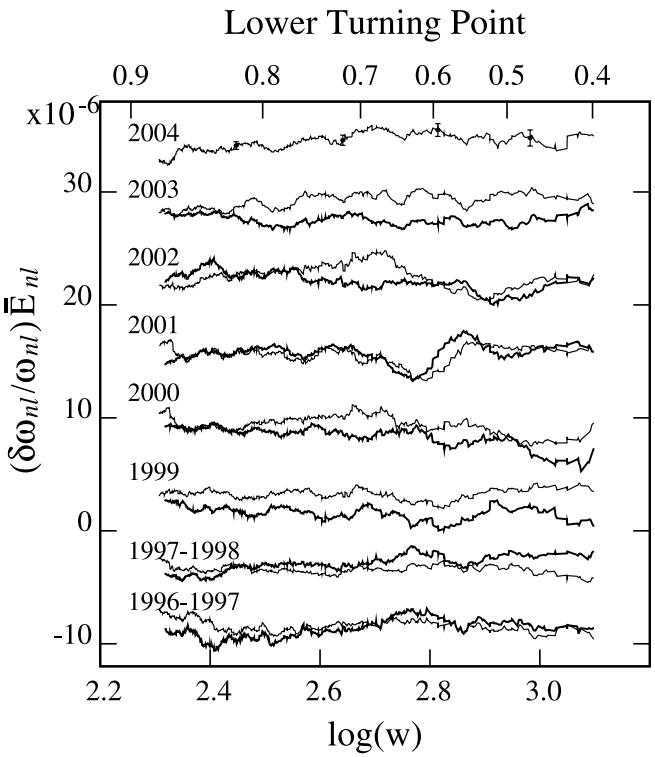

FIG. 4.—Smoothed $(\delta\omega_{nl}/\omega_{nl})\bar{E}_{nl}$ vs. $\log w$ for various periods along the solar cycle, using the frequency averaged over 1996.05–2003.12 as the reference. The MDI result is denoted by the thin lines, and the GONG one by the thick lines. All periods are independent. The period of 1996–1997 is 1996.05–1997.07. The period of 1997–1998 is 1997.07–1998.10. The curves of smoothed $(\delta\omega_{nl}/\omega_{nl})\bar{E}_{nl}$ are shifted to avoid interference: 1996–1997 by 4.7×10^{-5}, 1997–1998 by 2.5×10^{-5}, 1999 by -1.1×10^{-5}, 2000 by -2.3×10^{-5}, 2001 by -1.65×10^{-5}, 2002 by -0.85×10^{-5}, 2003 by 3.6×10^{-5}, and 2004 by 6.1×10^{-5}. The MDI and GONG curves are shifted by the same amount. The error bars for the curve for MDI 2004 at $\log w = 2.45$, 2.64, 2.81, and 2.98 are the errors of the 41 point running mean, computed with the errors of the measured frequencies, based on the error propagation.

The GONG results share the above properties of those of MDI. First, the curve of $(\delta\omega_{nl}/\omega_{nl})\bar{E}_{nl}$ versus w is flat in the period of low activity. The value of $(\delta\omega_{nl}/\omega_{nl})\bar{E}_{nl}$ at $\log w > 2.7$ decreases as magnetic activity increases, while it remains approximately constant at $\log w < 2.7$. Second, the magnitude of the difference between small and large w approximately correlates with the sunspot number, as shown in Figure 3. Despite these similarities, there exist discrepancies between GONG and MDI. First, the magnitude of $\langle(\delta\omega_{nl}/\omega_{nl})\bar{E}_{nl}\rangle_{\rm large} - \langle(\delta\omega_{nl}/\omega_{nl})\bar{E}_{nl}\rangle_{\rm small}$ for GONG is greater than that for MDI. The GONG value in Figure 3 is scaled by a factor of 2. The cause of this discrepancy is unknown.

The second discrepancy between GONG and MDI is that the MDI curve for 2003 is rather flat, while the GONG curve is not. The MDI curve for 2004 is also flat. The GONG frequency tables for 2004 were not available at the time this paper was written. It will be interesting to see whether the GONG curve for 2004 is flat or not. The quantitative discrepancies between GONG and MDI may be due to measurement errors and the different methods of determining the mode frequencies. The differences between the MDI and GONG pipelines to determine the mode frequencies are discussed in Schou et al. (2002). The two pipelines handle the spatial leakage differently. Both MDI and GONG use the symmetric Lorentzian line profile in the fit.

The effect of the error in the reference frequency would appear in the frequency change of every period. To minimize the

error in the reference frequency, we also use the frequency averaged over a longer period (1996.05–2003.12) as the reference frequency. Figure 4 shows solar cycle variations of smoothed $(\delta\omega_{nl}/\omega_{nl})\bar{E}_{nl}$ with the reference frequency averaged over 1996.05–2003.12. These curves are smoother than those using the frequency averaged over the minimum as the reference, but the feature of interest at $\log w \sim 2.7$ is little affected by the choice of reference, which strengthens its reliability.

To quantify the correlation between $\langle(\delta\omega_{nl}/\omega_{nl})\bar{E}_{nl}\rangle_{\rm large} - \langle(\delta\omega_{nl}/\omega_{nl})\bar{E}_{nl}\rangle_{\rm small}$ and the sunspot number shown in Figure 3, we compute their linear correlation coefficient (Press et al. 1999). The linear correlation coefficient is 0.89 for MDI and 0.92 for GONG. The significance (goodness of fit) of the linear fit of $\langle(\delta\omega_{nl}/\omega_{nl})\bar{E}_{nl}\rangle_{\rm large} - \langle(\delta\omega_{nl}/\omega_{nl})\bar{E}_{nl}\rangle_{\rm small}$ versus sunspot number is 0.84 for MDI and 0.37 for GONG (Press et al. 1999).

4. DISCUSSION

Figures 2–4 show that solar cycle variations of the w dependence of $(\delta\omega_{nl}/\omega_{nl})\bar{E}_{nl}$ for GONG and MDI are qualitatively similar rather than quantitatively similar. The qualitative consistency between GONG and MDI results is encouraging and strengthens the previous speculation in Paper I: the temporal variations of the difference in $(\delta\omega_{nl}/\omega_{nl})\bar{E}_{nl}$ between small w and large w may be associated with solar cycle variations of magnetic fields near the BCZ. The consistency between GONG and MDI results suggests that the signals detected here are unlikely to be caused by the systematic errors in measurements, because the instruments of the two projects are different. It is not clear whether the signals detected here are caused by the unknown systematic errors in data analysis shared by the MDI and GONG pipelines. For example, what are the systematic errors caused by fitting asymmetric line profiles with the symmetric Lorentzian profile?

The fact that the signals correlate with solar activities suggests the signals are associated with magnetic fields. We cannot rule out the possibility that these signals are the systematic effects caused by the oscillation data measured in and around the magnetic regions (Howe & Thompson 1998; Nicholas et al. 2004). However, it is not clear what kind of systematic effect would change $(\delta\omega_{nl}/\omega_{nl})\bar{E}_{nl}$ at large w while leaving it unchanged at small w.

We speculate that the signals detected here are caused by temporal variations of the physical conditions in a region near the BCZ. The model study in Paper I shows that the measured $(\delta\omega_{nl}/\omega_{nl})\bar{E}_{nl}$ could be explained by a change in adiabatic exponent, Γ_1 $(\equiv \partial \ln p/\partial \ln \rho|_s)$, in a region near the BCZ. The magnitude of $(\delta\omega_{nl}/\omega_{nl})\bar{E}_{nl}$ is approximately proportional to the product of the amplitude and width of $\delta\Gamma_1/\Gamma_1$. Comparison with the model study in Paper I suggests that the value of $(\delta\omega_{nl}/\omega_{nl})\bar{E}_{nl}$ measured with MDI frequencies corresponds to a perturbation of $-\delta\Gamma_1/\Gamma_1$ $(= -2\delta c/c) \approx (2\text{–}6)\times 10^{-5}$ at $r \approx 0.65\text{–}0.67\ R_\odot$, if the FWHM of the Gaussian perturbation is $0.05\ R_\odot$. The amplitude of $\delta\Gamma_1/\Gamma_1$ corresponding to the GONG results is about twice the MDI amplitude.

We thank Sushanta C. Tripathy for providing the frequency tables of GONG and Jesper Schou for providing the frequency tables of *SOHO* MDI. This work uses data obtained by the Global Oscillation Network Group (GONG) program, managed by the National Solar Observatory, which is operated by AURA, Inc., under a cooperative agreement with the National Science Foundation. The data were acquired by instruments operated by the Big Bear Solar Observatory, High Altitude Observatory, Learmonth Solar Observatory, Udaipur Solar Observatory, Instituto de Astrofísica de Canarias, and Cerro Tololo Interamerican Observatory. *SOHO* is a project of international cooperation between ESA and NASA. A. S. was supported by a NATO/NSF grant. D. Y. C. was supported by NSC of Taiwan under grant NSC-93-2112-M-007-026.

REFERENCES

Antia, H. M., Basu, S., Hill, F., Howe, R., Komm, R. W., & Schou, J. 2001, MNRAS, 327, 1029
Basu, S., & Antia, H. M. 2002, in Proc. *SOHO* 12/GONG 2002 Workshop, Local and Global Helioseismology, ed. H. Sawaya-Lacoste (ESA SP-517; Noordwijk: ESA), 231
Basu, S., Christensen-Dalsgaard, J., Howe, R., Schou, J., Thompson, M. J., Hill, F., & Komm, R. 2003, ApJ, 591, 432
Basu, S., & Schou, J. 2000, Sol. Phys., 192, 481
Chaplin, W., Elsworth, Y., Isaak, G. R., Lines, R., McLeod, C. P., Miller, B. A., & New, R. 1998, MNRAS, 298, L7
Chou, D.-Y., & Dai, D.-C. 2001, ApJ, 559, L175
Chou, D.-Y., & Ladenkov, O. 2005, ApJ, 630, 1206
Chou, D.-Y., & Serebryanskiy, A. 2005, ApJ, 624, 420 (Paper I)
Christensen-Dalsgaard, J., Duvall, T. L., Jr., Gough, D. O., Harvey, J. W., & Rhodes, E. J., Jr. 1985, Nature, 315, 378
Christensen-Dalsgaard, J., Gough, D. O., & Perez Hernandez, F. 1988, MNRAS, 235, 875
Eff-Darwich, A., Korzennik, S. G., Jimenez-Reyes, S. J., & Perez Hernandez, F. 2002, ApJ, 580, 574
Elsworth, Y., Howe, R., Isaak, G. R., McLeod, C. P., Miller, B. A., New, R., Speake, C. C., & Wheeler, S. J. 1994, ApJ, 434, 801
Harvey, J. W., et al. 1996, Science, 272, 1284
Howe, R., Christensen-Dalsgaard, J., Hill, F., Komm, R., Larsen, R. M., Schou, J., Thompson, M. J., & Toomre, J. 2000, Science, 287, 2456
Howe, R., Komm, R., & Hill, F. 1999, ApJ, 524, 1084
———. 2002, ApJ, 580, 1172
Howe, R., & Thompson, M. J. 1998, A&AS, 131, 539
Jain, K., & Bhatnagar, A. 2003, Sol. Phys., 213, 257
Jimenez, A. 2002, ApJ, 581, 736
Libbrecht, K. G., & Woodard, M. F. 1990, Nature, 345, 779
Nicholas, C. J., Thompson, M. J., & Rajaguru, S. P. 2004, Sol. Phys., 225, 213
Press, W. H., Teukolsky, S. A., Vetterling, W. T., & Flannery, B. P. 1999, Numerical Recipes in C (2nd ed.; Cambridge: Cambridge Univ. Press), chaps. 14, 15
Regulo, C., Jimenez, A., Palle, P. L., Perez Hernandez, F., & Roca Cortes, T. 1994, ApJ, 434, 384
Rhodes, E. J., Jr., Cacciani, A., Korzennik, S. G., & Ulrich, R. K. 1993, ApJ, 406, 714
Scherrer, P. H., et al. 1995, Sol. Phys., 162, 129
Schou, J. 1999, ApJ, 523, L181
Schou, J., et al. 2002, ApJ, 567, 1234
Shibahashi, H. 1991, in Challenges to Theories of the Structure of Moderate-Mass Stars, ed. D. Gough & J. Toomre (Berlin: Spinger), 101
van der Linden, R. A. M., et al. 2005, Online Catalogue of the Sunspot Index (Brussels: Royal Observatory of Belgium), http://sidc.oma.be/html/sunspot.html
Woodard, M. F., Libbrecht, K. G., Kuhn, J. R., & Murray, N. 1991, ApJ, 373, L81